



Research Article / Araştırma Makalesi
EVAPORATIVE HEAT TRANSFER AND PRESSURE DROP OF R410A AND R32 IN SMOOTH HORIZONTAL TUBE

Alihsan KOCA*, Zafer GEMİCİ

Mir Research and Development Inc., İSTANBUL

Received/Geliş: 28.05.2013 Revised/Düzelme: 24.07.2013 Accepted/Kabul: 02.09.2013

ABSTRACT

Flow boiling heat transfer of R410A and R32 inside a smooth horizontal tube whose hydraulic diameters are 5,6 and 7mm. The mass flux was varied from 100 to 400 kg/m^2s , heat flux from 5 to 15 kj/m^2h , as the saturation temperature were maintained at -30 °C and -40 °C. The effects of the imposed wall heat flux, mass flux, vapor quality on the evaporation heat transfer and pressure drop discussed as a function of vapor quality and tube length. The results from Matlab program are compared with experimental data.
Keywords: R410, A R32, heat transfer, pressure drop, horizontal tube.

YATAY TÜPTE R410A VE R32 SOĞUTUCU AKIŞKANLARININ BASINÇ DÜŞÜŞÜ VE BUHARLAŞMA ISI TRANSFERİNİN İNCELENMESİ

ÖZET

Çapı 5,6 ve 7 mm olan yatay bir tüpte R410A ve R32 soğutucu akışkanlarının kaynamalı akış ısı transferi incelenmiştir. Çalışmada akışkan doyma sıcaklığı -30°C ve -40 °C olduğu durumlarda kütle akısının 100 ile 400 kg/m^2s , ısı akısının 5 ile 15 kj/m^2h arasında değiştiği durumlar incelenmiştir. Isı akısı, kütle akısı, buhar kalitesi parametrelerinin buharlaşma ısı transfer katsayısı ve basınç kaybına etkisi buhar kalitesi ve yatay boru uzunluğunun fonksiyonu olarak incelenmiştir. Matlab programında hesaplanan değerler literatürdeki deneysel sonuçlarla karşılaştırılmıştır.

Anahtar Sözcükler: R 410 A, R32, Isı Transferi, Basınç düşüşü, Yatay tüp.

1. INTRODUCTION

Refrigerant R410A, which is mixture of 50% R32 and 50% R125 by mass, is one of the most likely substitutes for R22 in residential applications. Although there have been extensive studies related to the performance of heat exchanger with R410A, investigations on two-phase heat transfer coefficient and pressure drop inside the heat exchangers have been limited.

Yongchan Kim (1986) he studied the evaporation heat transfer characteristics of R410A in the 9.52 and 7mm OD micro-fin/smooth tubes were measured at the evaporating temperatures of -15, -5 and 5 °C, the mass flux from 70 to 211 kg/m^2s , and the heat flux from 5 to 15 kW/m^2 . In his work the effects of heat flux, mass flux, evaporating temperature, and tube

*Corresponding Author/Sorumlu Yazar: e-mail/e-ileti: ihsankoca@dizayngrup.com, tel: (212) 886 57 41

diameter on the evaporation heat transfer coefficient were investigated. His experimental results showed that the evaporation heat transfer coefficient increased with heat flux and mass flux for all the tubes tested. It was also observed that for 7.0 mm OD tubes the average evaporation heat transfer coefficients increased as the evaporating temperature dropped at the low heat flux (5 kW/m^2).

C.Y. Park, P.S. Hrnjak (2007) investigated flow boiling heat transfer coefficient, pressure drop and flow pattern in the horizontal smooth tube of 6.1 mm inner diameter for CO₂, R410A and R22.

A.Greco, G.P. Vanoli (2005) indicated that the heat transfer coefficients increase with saturation pressure and heat flux at a fixed refrigerant mass flux.

Jatuporn Kaew-On (2009) in his work the heat transfer coefficient and pressure drop of R410A is investigated. The effects of mass flux, heat flux and saturation temperature on the heat transfer coefficient are also determined. The range of mass flux and heat flux in his work are 200-400 $\text{kg/m}^2 \text{ s}$ and 5-14 kW/m^2 respectively.

According to his work: the average heat transfer coefficient of R410A during evaporation tended to increase with increasing the average quality, mass flux but tended to decrease with increasing saturation temperature. The pressure drop increased with increasing the mass flux, but decrease with saturation temperature, and the heat flux has no significant effect on the pressure drop. Choi et. al (2002) presented boiling heat transfer coefficients of R-410A in tubes with inner diameters of 1.5 and 3.00 mm, explaining the effects of the tube diameter on the boiling heat transfer coefficient.

Rin Yun, Jae Hyeok Heo (2006) studied evaporative heat transfer and pressure drop of R-410A in micro channels, and reported the effects of saturation pressure, mass flux and heat flux on the heat transfer coefficient.

Chang et. al (2000) reported two phase pressure drops of R410A in a 5 mm tube. They proposed a modified Friedel Correlation, which extended the capability of the Friedel correlation to a small diameter tube.

The objectives of the present study are to provide extended data by computer program on heat transfer and pressure drop for R410A flowing inside a smooth horizontal tube.

2. THEORETICAL ANALYSIS

The following assumptions are made:

- 1-The coolant enters to the evaporator as a saturated liquid and leaves as a saturated vapor.
- 2-In our model the tube is smooth and horizontal.
- 3- Evaporation occurs at the saturation temperature.
- 4-Phases are dispersed uniform among each other.
- 5-Both faces have the same velocity.

With knowledge of the input heat flux, diameter of tube, mass flux and saturation temperature, the mass qualities x at measurement locations z were calculated from heat balances based on φ as follows:

$$\frac{dq_e}{dz} = \pi \cdot D \cdot \varphi \quad (1)$$

Where φ is heat flux over heated length.

By defining

$$\dot{m} \frac{dh}{dz} = \pi \cdot D \cdot \varphi \quad (2)$$

$$\frac{dh}{dz} = \frac{dx}{dz} h_{lv} \quad (3)$$

Combining equations (1), (2) and (3), we obtain

$$x(z) = x_{in} + \frac{4\varphi}{G.D.h_{lv}} .z \quad (4)$$

The length of two-phase flow region was determined by iteration from the equation (4). Where h_{lv} phase-change enthalpy (kJ.kg^{-1}), φ heat flux (W.m^{-2}), D diameter (m), x vapor quality, z axial length (m)

2.1. Heat Transfer Analysis

The boiling heat transfer is a very important design parameter to heat exchanger designers because the evaporator or boiler performance strongly depends on the flow boiling. In the literature two methods are commonly found as the form of two phase heat transfer correlation. The first, similar to the two phase pressure drop correlations, uses a two phase multiplier to express the two phase heat transfer in terms of the single phase liquid heat transfer. The second type is a super position method that combines convective and nucleate boiling terms to compute the two phase heat transfer coefficient. In this study the two phase multiplier heat transfer correlation used which is developed by Gungor and Winterton (1986) which is given by:

$$h_{tp} = E.h_l \quad (5)$$

$$E = 1 + 3000Bo^{0.86} + \left(\frac{x}{1-x}\right)^{0.75} \left(\frac{\rho_l}{\rho_v}\right)^{0.41} \quad (6)$$

The single phase liquid heat transfer coefficient h_l is calculated by the Dittus-Boelter correlation.

$$h_l = 0.023 \cdot \left(\frac{k_l}{D_h}\right) \text{Re}_l^{0.8} \cdot \text{Pr}_l^{0.4} \quad (7)$$

$$\text{Re}_l = \frac{G \cdot (1-x) D_h}{\mu_l} \quad (8)$$

$$Bo = \frac{q''}{G.h_{lv}} \quad (9)$$

Where Bo Bond number, D_h hydraulic diameter, (m) k_l thermal conductivity, ($\text{W.m}^{-1}.\text{K}^{-1}$).

2.2. Pressure Drop Analysis

The knowledge of pressure drop in a two-phase flow system is also important for its design. It enables the designer to size the pump required for the operation of the flow system.

2.2.1. Homogeneous Fluid Model

The pressure gradient in a two-phase flow can be thought of as arising from three additive contribution: (i) frictional (ii) flow acceleration (iii) hydrostatic head.

Thus,

$$\frac{dp}{dz} = \left(\frac{dp}{dz}\right)_{fr} + \left(\frac{dp}{dz}\right)_{ac} + \left(\frac{dp}{dz}\right)_{gr} \tag{10}$$

In the homogeneous fluid model, the fluid is characterized by an effective fluid that has suitably averaged properties of the liquid and gas phases.

2.2.1.1. Pressure drop due to flow acceleration

The pressure gradient due to flow acceleration can be written as

$$\left(\frac{dp}{dz}\right)_{ac} = \frac{d}{dz} \left(\frac{1}{A} \int_A \rho u^2 dA \right) = G \frac{d}{dz} \left(\frac{1}{\rho_H} \right) \tag{11}$$

Where G is the total rate of mass flow per unit area in the tube, and the effective density ρ_H is defined by:

$$\rho_H = \frac{1}{(\mathcal{G}_l + x\mathcal{G}_v)} \tag{12}$$

After assumption and integration through the tube we may write

$$\Delta P_{ac} = G^2 \cdot \mathcal{G}_v \cdot x \tag{13}$$

2.2.1.2. Pressure drop due to gravity

The pressure gradient due to gravity may be written as

$$\left(\frac{dp}{dz}\right)_{gr} = g_z \cdot \rho_M = \frac{g_z}{(\mathcal{G}_l + x\mathcal{G}_v)} \tag{14}$$

After integration of equation (14) we arrive,

$$\Delta P_{gr} = \frac{g_z \cdot L}{\mathcal{G}_l \cdot x} \cdot \ln \left[1 + x \cdot \frac{\mathcal{G}_v}{\mathcal{G}_l} \right] \tag{15}$$

2.2.1.3. Pressure drop due to wall friction

The frictional pressure drop due to the shear stress exerted by the tube wall is considered the most problematic term in two-phase pressure drop. The frictional pressure drop may be related to the wall stress τ_w by a force balance:

$$\left(\frac{dp}{dz}\right)_{fr} = \frac{2\tau_w}{R} \tag{16}$$

$$\left(\frac{dp}{dz}\right)_{fr} = \frac{f \cdot \dot{m}^2}{\rho_H \cdot R} \quad (17)$$

After integration of equation (17) we arrive

$$\Delta P_{fr} = \frac{2 \cdot f_p \cdot L \cdot G^2 \cdot \mathcal{G}_l}{D} \left[1 + \frac{x_{out}}{2} \left(\frac{\mathcal{G}_{lv}}{\mathcal{G}_l} \right) \right] \quad (18)$$

$$f = 0.079 \cdot \text{Re}^{-0.25} \quad (19)$$

Where the Reynolds number is $\text{Re} = \frac{2\dot{m}R}{\mu_H}$

$$\frac{1}{\mu_H} = \frac{x}{\mu_V} + \frac{(1-x)}{\mu_L} \quad (20)$$

Where A surface area (m²), P pressure (kPa), g gravitational constant (m.s⁻²), f frictional factor, v specific volume (m³.kg⁻¹), u velocity (m.s⁻¹), R radius (m), \dot{m} mass flow rate (kg.s⁻¹), q' heat flux (W.m⁻²), D_h hydraulic diameter (m)

2.2.2. Separated Flow Model

In this model the flow of the gas and vapor are analyzed as though the gas and liquid streams flow through separate tubes, with cross-section area proportional to the void fraction.

2.2.2.1. Pressure drop due to flow acceleration

The pressure gradient due to flow acceleration may be written as follows,

$$\left(\frac{dp}{dz}\right)_{ac} = \frac{d}{dz} \left(\frac{1}{A} \int_A \rho \cdot u^2 dA \right) = \dot{m}^2 \frac{d}{dz} \left(\frac{x^2}{\rho_V \cdot \alpha_M^2} + \frac{(1-x)^2}{\rho_L (1-\alpha_M)^2} \right) \quad (21)$$

2.2.2.2. Pressure drop due to gravity

The expression for the pressure drop due to gravity is the same as that give for the homogeneous model.

2.2.2.3. Pressure drop due to wall friction

Lockhart-Martinelli correlation

The Lockhart-Martinelli correlation (1945) for two-phase pressure gradient is similar in idea to the two-phase multiplier. A parameter X is defined as

$$X^2 = \frac{(dp/dz)_{LP}}{(dp/dz)_{VP}} \quad (22)$$

Which is the ratio of the frictional pressure gradients for the liquid and gas alone, flowing at their respective superficial velocities. The single phase pressure drops are obtained using the equation that uses a friction factor:

$$\frac{dp}{dz} = \frac{f \cdot \rho \cdot u^2}{R} \quad (23)$$

Where $f = \frac{16}{Re}$ for laminar flow,

And for turbulent flow, two correlations are used:

$$f = \frac{0,079}{Re^{0,25}} \quad Re \leq 2 \times 10^4, \text{ or} \quad (24)$$

$$f = \frac{0,046}{Re^{0,2}} \quad Re \geq 2 \times 10^4 \quad (25)$$

Where Re is based on pipe diameter $Re = \frac{\rho U \cdot D}{\mu}$ [7].

The two-phase frictional pressure gradient is then obtained by a multiplier defined as

$$\left(\frac{dp}{dz} \right)_{fr} = \phi_G^2 \left(\frac{dp}{dz} \right)_{GS} = \phi_L^2 \left(\frac{dp}{dz} \right)_{LS} \quad (26)$$

$$\phi_G = 1 + CX + X^2 \quad \phi_L = 1 + CX^{-1} + X^{-2} \quad (27)$$

Where C is empirically determined and is in range $5 < C < 20$. The value of C is 5 when the flow of liquid and gas is laminar and 20 when both flows are turbulent.

Where, X Martinelli parameter, X_{tt} Martinelli parameter for turbulent-turbulent flow,

3. RESULTS

In this study Matlab Program is used to calculate the flow boiling heat transfer coefficient and two-phase pressure drops of R410A and R32 with general correlation inside a smooth horizontal tube whose hydraulic diameters are 5, 6 and 7 mm. The mass flux was varied from 100 to 300 kg/m^2s , heat flux from 5 to 15 kJ/m^2h , as the saturation temperature were maintained at -30 °C and -40 °C.

Gungor and winterton (1986) correlation is used to predict the flow boiling heat transfer coefficient and the prediction of pressure drop is performed by the homogenous and Lochart-Martinelli (1949) models.

The effects of the imposed wall heat flux, mass flux, tube diameter and saturation temperature on the evaporation heat transfer and pressure drop discussed as a function of vapor quality and tube length. Then results from computer program are compared with experimental data.

3.1. Heat Transfer Predictions of R410A

In this study, the flow boiling heat transfer coefficients are calculated for R410A and R32. Before calculate these refrigerants, it is necessary to compare the calculated R410A flow boiling heat transfer coefficients with previous studies for comparison of the calculation accuracy of the program in this study. The experimental conditions are summarized in table 1.

Table 1. Summary of experimental conditions for two-phase flow heat transfer coefficient

Reference	G (kg/m ² s)	D _{tube} (mm)	q'' (kj/ m ² s)	T _{sat} (°C)
Kim et al. [1]	164	6.1	5	-15
C.Y. Park, P.S. Hrnjak [2]	400	6	5	-15
Ebusi and Torikoshi [9]	150	7	7.5	5

Table 2. Summary of experimental conditions for two-phase flow pressure drop

Reference	G (kg/m ² s)	D _{tube} (mm)	q'' (kj/ m ² s)	T _{sat} (°C)
Jatuporn Kaew-On	200	5	10	30
Jatuporn Kaew-On	400	5	10	10

Park and Hrnjak (2005), Kim et al. (2002) and Ebusi and Torikoshi (1998) used the Gungor and Winterton (1986) correlation to predict heat transfer coefficient for R410A.

Figure 1 shows the comparison of heat transfer coefficients for R410 in this study with Kim (2002) with a bias error -13 % and 1 % at similar condition. As shown in the figure the program data for 6.1 mm smooth tubes were reasonable consistent with the data obtained from the literature excluding the Kim et al. (2002) data.

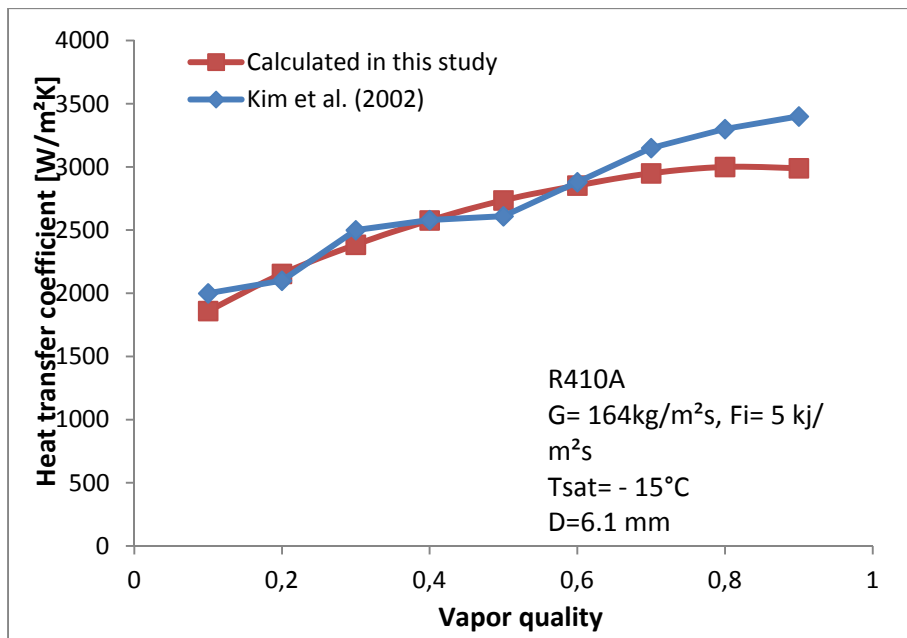


Figure 1. Comparison of heat transfer coefficients for R410A in this study with Kim et al.[1]

However the little deviation seems to be caused by the difficulty of experimental measurement. As seen in Figure 2 the deviation became higher with the reason of more difficult visualization of the vapor than the liquid. Another reason is of the deviation is measurement sensibility of the experimental apparatus.

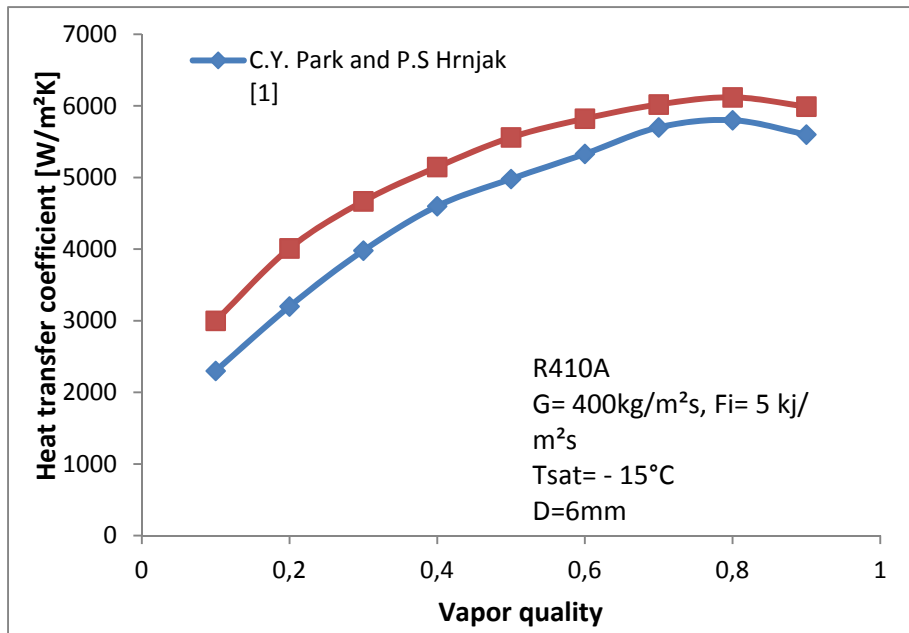


Fig. 2. Comparison of heat transfer coefficients for R410A in this study with Park and Hrnjak [2]

Figure 2 and 3 show the comparison between the calculated heat transfer coefficients by Gungor and Winterton (1986) correlation and other studies developed by Park and Hrnjak (2005) with a bias error 4.6 % and 18 %, Ebisu and Torikoshi (1998) with a bias error 1.2 % and 21 %, respectively.

Calculated heat transfer coefficients for R410A show the higher heat transfer coefficients for every test conditions of Gungor and Winterton (1986) in Figs. 2 This trend demonstrates that the convective boiling is significantly active heat transfer mechanism for R410A. Whereas, the enhancement of heat transfer coefficients with the increase of mass flux and quality is not significant for R410A because of the nucleate boiling dominance on R410A flow boiling heat transfer

In the higher vapor quality differences between the calculated heat transfer coefficient and measured data studied by Ebusi and Torikoshi (1998) increasing in Figs. 3. This trend can be explained by the difference of the density ratio of liquid to vapor for, R410A. Convective boiling is usually enhanced by the increasing of the average velocities of liquid and vapor as the quality increases. As the density ratio of liquid to vapor decreases, there is a higher variation in the convective boiling heat transfer coefficient as quality increases due to the smaller change in the liquid and vapor average velocities.

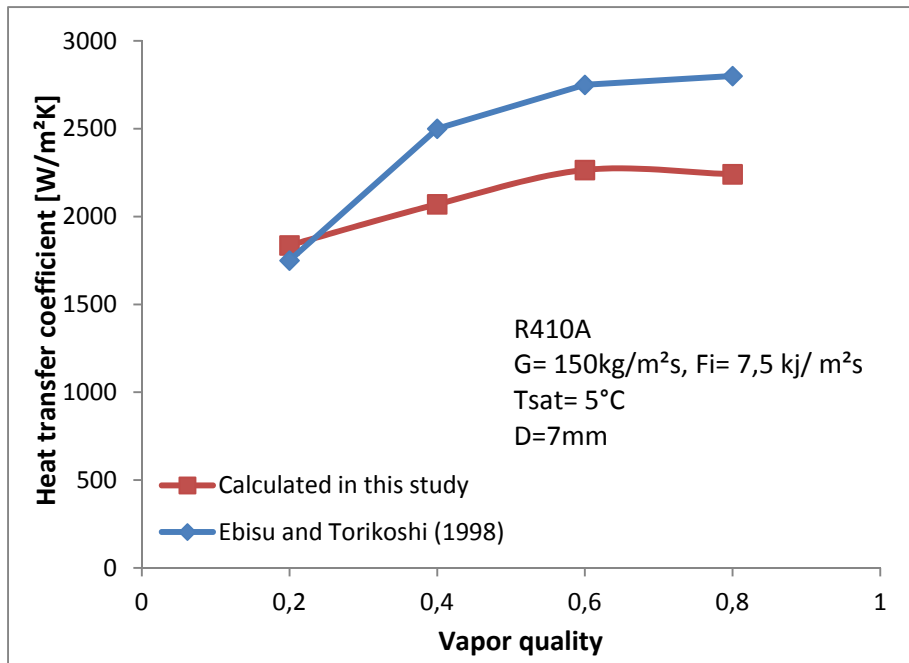


Fig. 3. Comparison of heat transfer coefficients for R410A in this study with Ebisu and Torikoshi [9]

Figure 4 shows the heat transfer coefficient comparison for R410A and R32 at an evaporation temperature of $-40\text{ }^{\circ}\text{C}$, heat flux of $10\text{ }kj/m^2s$ and mass flux variation from 100 to $300\text{ }kg/m^2s$. The heat transfer coefficients of R32 are much higher than those of R410A.

As presented figure 4, the heat transfer coefficient for R410A and R32 increase significantly as the quality increase. Convective boiling is usually enhanced by the increasing of the average velocities of liquid and vapor as the quality increase. As the density ratio decrease, there is a smaller variation in the convective boiling heat transfer coefficient as quality increases due to the smaller change in the liquid and vapor average velocities.

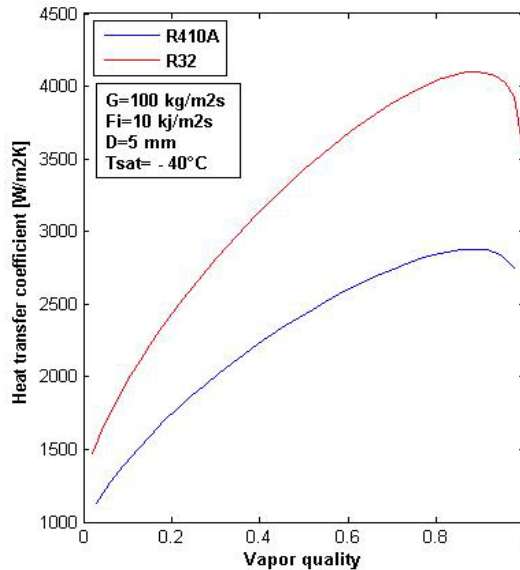


Figure 4. Comparison heat transfer coefficient of R410A and R32 with respect to quality

Figure 5 shows the flow boiling heat transfer coefficients for R410A at evaporation temperatures of -30 and -40 °C, at a mass flux of $100 \text{ kg/m}^2\text{s}$ and heat flux of $10 \text{ kJ/m}^2\text{s}$ for the 5 mm tube. The flow boiling heat transfer coefficient for R410A at the evaporation temperature of -40 °C are higher than those at -30 °C. This is because the heat transfer rate might be reduced by the lower vapor shear due to a decrease in vapor velocity at the vapor- liquid interface according at higher temperatures. Another proposed reason is that heat transferred through the liquid annulus in annular flow pattern depends on the thermal conductivity of liquid film. This results in a decrease of the heat transfer coefficient as the vaporization temperature is increased.

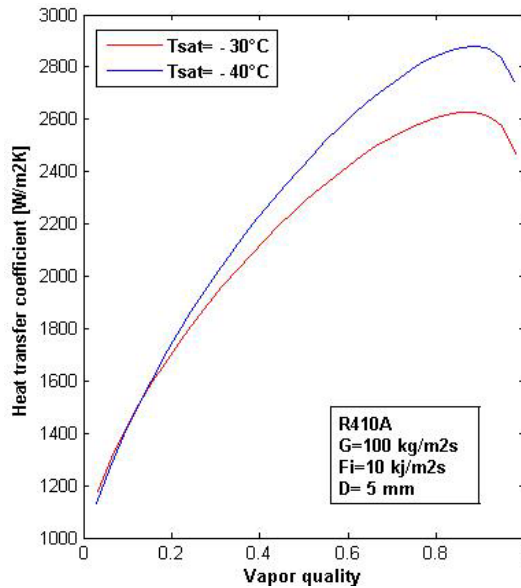


Figure 5. Effect of saturation temperature on the heat transfer coefficient

Figure 6 shows the variation of the heat transfer coefficient versus average quality during evaporation of R410A at $T_{sat} = -40\text{ }^{\circ}\text{C}$ for different mass fluxes of 100, 200 and 300 $\text{kg}/\text{m}^2\text{s}$ and heat flux of 10 $\text{kJ}/\text{m}^2\text{s}$. As shown, the heat transfer coefficient increases with increasing mass flux. However, at very low average there is lower effect of mass flux on the heat transfer coefficient. At all mass fluxes of refrigerant, the heat transfer coefficient tends to increase with increasing the quality. The heat transfer coefficient increases slightly with increasing average quality until the maximum heat transfer coefficient is reached, then decreases with increasing quality. This can be explained as follows:

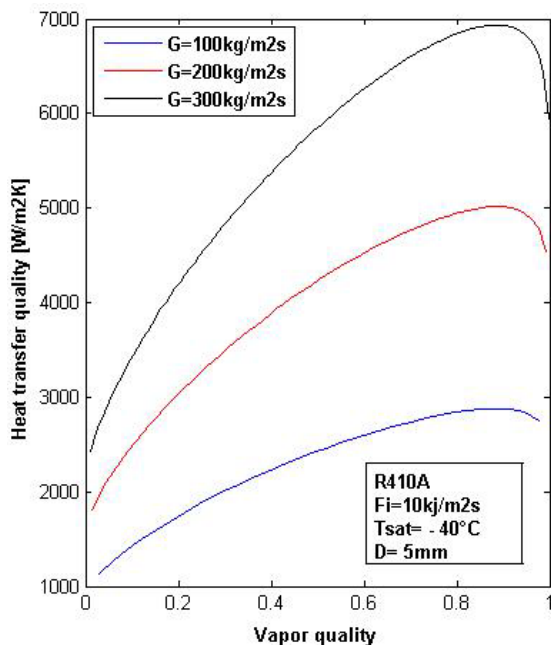


Figure 6. Heat transfer coefficient of R410A with respect to mass fluxes and quality

Firstly, during evaporation, the liquid refrigerant boiled and turned to vapor, which has higher specific volume than liquid. This led to an increase in the velocity of two-phase flow, which resulted in the increase of heat transfer coefficient.

Secondly, as the average quality increased, the liquid film thickness decreased, which then reduced the thermal resistance in the liquid film and a higher heat transfer coefficient is obtained.

3.2. Pressure Drop Predictions of R410A

In this study two phase pressure drops of R410A and R32 for 5, 6 and 7 mm tubes are calculated with general correlations for macro scale tubes. The prediction of pressure drop is performed by the homogenous and Lochart-Martinelli (1949) models. The saturation temperatures for the pressure drop are -30 and -40 °C and vapor quality is varied from 0 to 1. The mass fluxes are 100, 200 and 300 $kg/m^2 s$.

Figure 7 and 8 show the comparison between the calculated frictional pressure drop from the correlation of Lochart-Martinelli (1949) and Jatuporn Kaew-On's (2009) experimental data's.

Figure 7 and 8 show the comparison between the calculated frictional pressure drop from the correlation of Lochart-Martinelli (1949) and Jatuporn Kaew-On's (2009) experimental data's.

Figure 7 shows the distribution of Jatuporn (2009) and the results of computer program pressure drop predictions for R410A with a bias error 36% and -12%, respectively.

Figure 8 shows the distribution of Jatuporn (2009) and the results of computer program pressure drop predictions for R410A with a bias error -13,6% and -3.3%, respectively.

Calculations in this study can give good agreement with the measured pressure drop as seen in the Figure 8. However the little deviation can be explained as follows; In the experimental study of Jatuporn (2009) the evaporation pressure drop was measured by the differential pressure transducer mounted to the header at inlet and outlet of the test section. The total pressure drop includes the sudden contraction loss at the test section inlet, sudden expansion loss at the test section outlet, frictional pressure drop, and acceleration pressure drop. The results from the experimental study shows that the frictional pressure drop is 73– 95% of the total pressure drop.

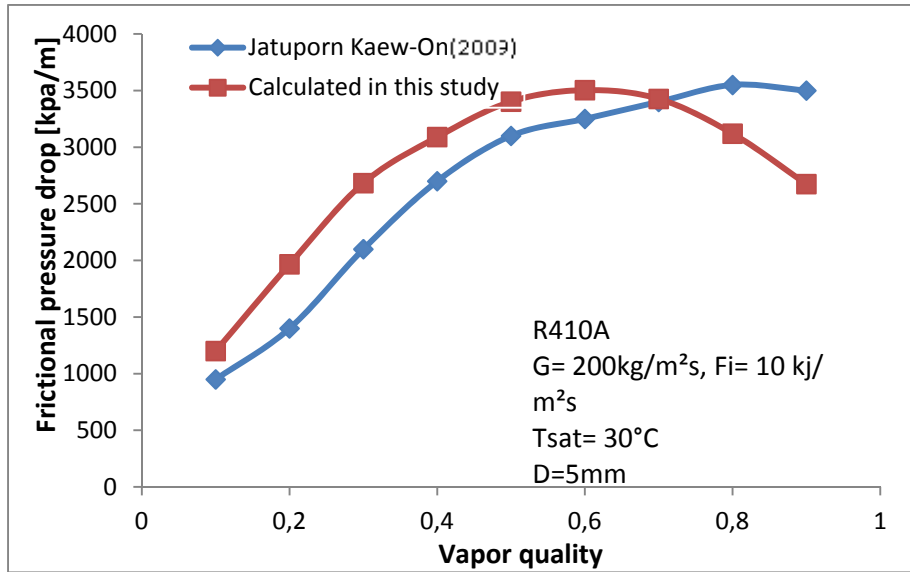


Figure 7. Comparison of calculated pressure drop with Jatuporn [4]

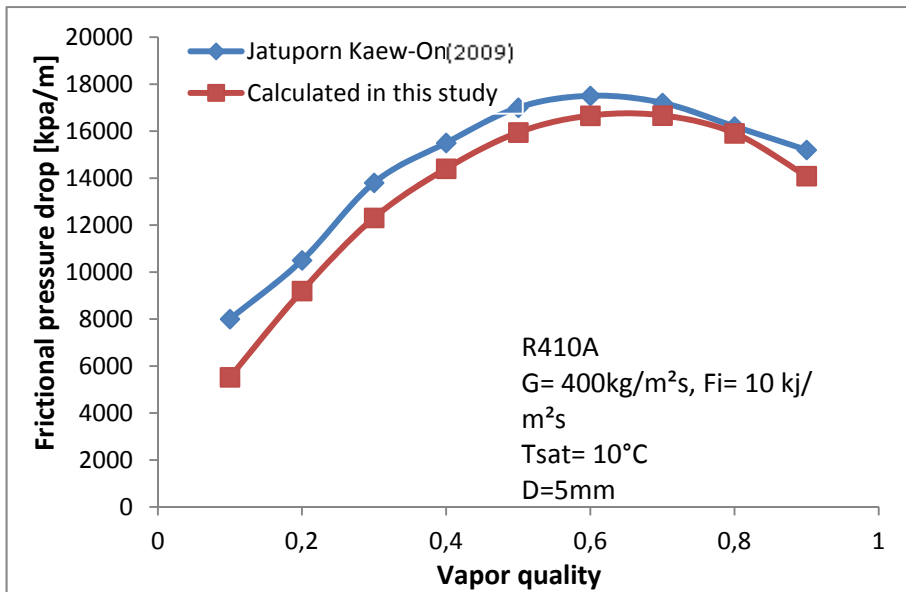


Figure 8. Comparison of calculated pressure drop with Jatuporn [4]

3.2.1. Effects of Mass Flux on Frictional Pressure Drop

The frictional pressure drops versus heat flux during evaporation of R410A and R32 at constant saturation temperature were calculated by the homogenous and Lochart-Martinelli models.

Fig. 9, 10 and show the effects of the mass flux on the pressure drop for the 5 mm OD at a heat flux of 10 $\text{kJ/m}^2\text{s}$.

As shown, the frictional pressure drop increases with the average quality. At the same quality, the pressure at higher mass flux is always higher than at lower ones across the range of quality.

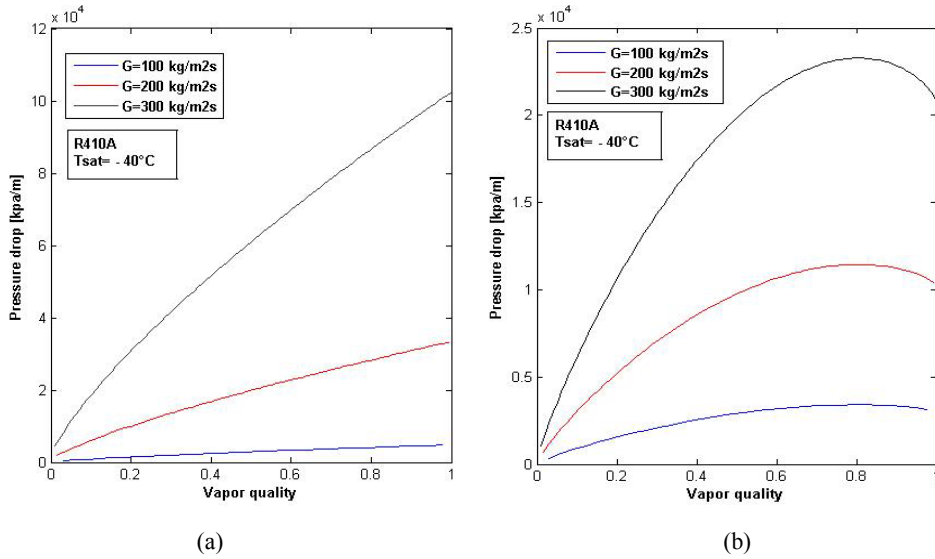


Figure 9. Pressure drop of R410A according to the (a) homogenous and (b) separated flow model

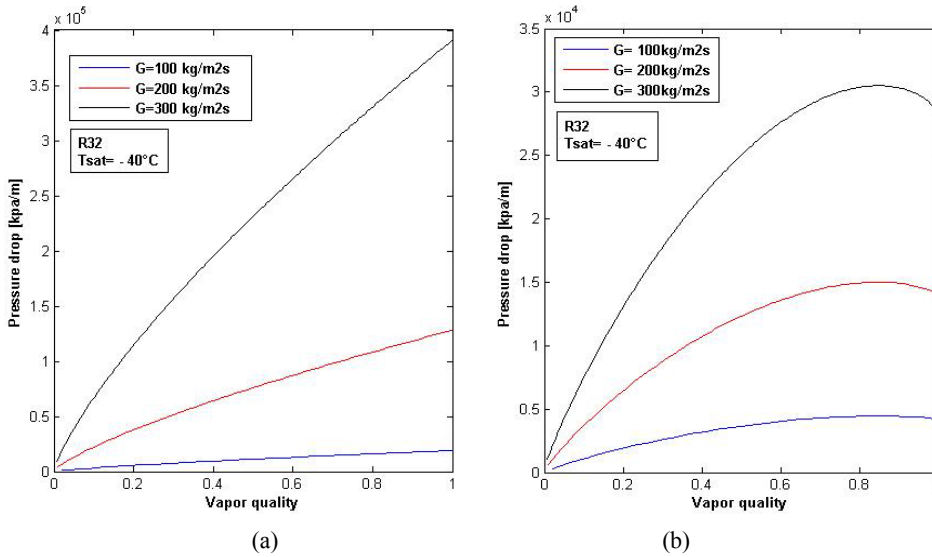


Figure 10. Pressure drop of R32 according to the (a) homogenous and (b) separated flow model

According to the both models pressure drops of R32 are always higher than R410A.

3.2.2. Effects of Heat Flux on Frictional Pressure Drop

Figure 11 presents the variation of the pressure drop with the quality at $G = 100 \text{ kg/m}^2 \text{ s}$ and $T_{\text{sat}} = 40^\circ \text{C}$ for the different heat flux values of 5, 10 and 15 $\text{kJ/m}^2 \text{ s}$

On the Lochart-Martinelli model it is found that the heat flux has no significant effect on the pressure drop. This is because the increase in the total rate of liquid film vaporization in the wall surface is very small with the vapor flow rate at the inlet.

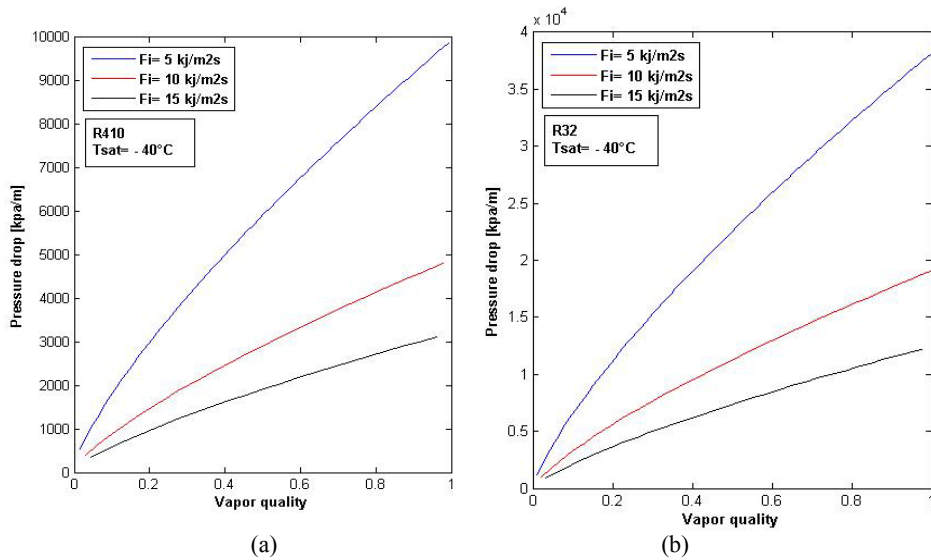


Figure 11. Effects of heat flux on frictional pressure drop for (a) R410A (b) R32

3.2.3. Effects of Saturation Temperature on the Frictional Pressure Drop

Figure 12 shows the effects of the evaporating temperature on the pressure drop per unit length for the 5 mm OD smooth tube at a mass flux of $100 \text{ kg/m}^2 \text{ s}$ and heat flux $10 \text{ kJ/m}^2 \text{ s}$. The pressure drop increased with the rise of the evaporating temperature.

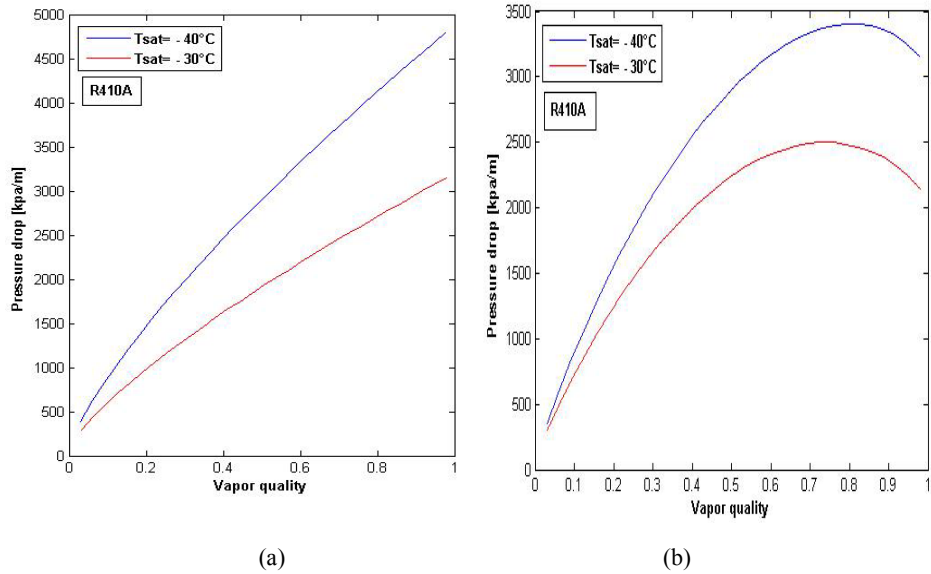


Figure 12. Effects of saturation temperature for (a) homogeneous and (b) Lochart-Martinelli model on the frictional pressure drop.

3.2.4. Effects of Tube Diameter on the Frictional Pressure Drop

The diameter of tube gives a considerable effect on two-phase flow pressure drop, and figure 13 shows the effects on R410A pressure drop for the saturation temperature of -40°C at the mass flux 100 and $300\text{ kg/m}^2\text{s}$ for the tube diameter 5 and 7 mm. The pressure drop increase with the decrease of tube diameter.

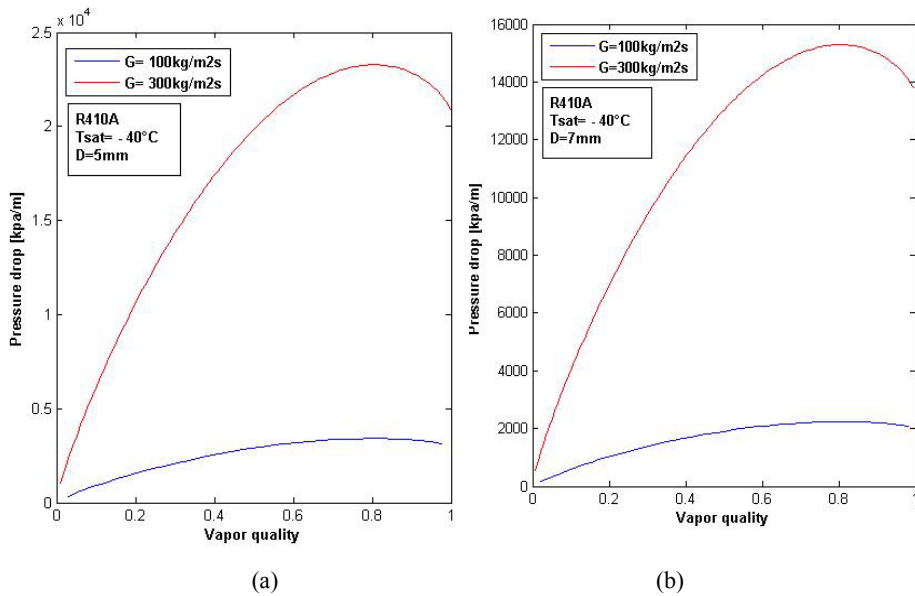


Figure 13. Effects of tube diameter for Lockhart-Martinelli model on the frictional pressure drop (a) $D=5\text{mm}$ (b) $D=7\text{mm}$.

NOMENCLATURE

Greek symbols

- α void fraction
- μ viscosity, $\text{N}\cdot\text{s}\cdot\text{m}^{-2}$
- ρ density, $\text{kg}\cdot\text{m}^{-3}$
- σ surface tension, $\text{N}\cdot\text{m}^{-1}$
- τ_w Perimeter average shear stress, Pa

Subscript

- ac accelerational
- fr friction
- gr gravitational
- in inlet
- l liquid
- lp liquid-phase
- lv property difference between vapor and liquid
- o outlet
- ref refrigerant
- sat saturation
- tp two-phase
- v vapor
- vp vapor-phase
- w wall

REFERENCES / KAYNAKLAR

- [1] Chang, Y.J. Chiang, S.K. Chung, T.W. Wang, C.C. Two-phase frictional characteristics of R410A and air-water in a 5 mm smooth tube, *ASHREA Trans.* 106 (1) (2000) 792-797.
- [2] Choi K.I., Pamitran, J.T. Oh, Boiling heat transfer of R410A in horizontal small diameter tubes, *Proceedings of 2002 winter annual conference, The Society of Air-Conditioning and Refrigerating Engineers of Korea*, (2002), [p.283-288].
- [3] Ebisu, T. Torikoshi, K. Heat transfer characteristics and correlations for R410A flowing inside a horizontal smooth tube, *ASHREA Trans.* 104 (2) (1998), 556-561.
- [4] Greco A., Vanoli, G.P., Flow boiling heat transfer with HFC mixtures in a smooth horizontal tube, *Experimental Thermal Fluid Science* 29 (2005), 716-730.
- [5] Gungor, K.E., Winterton, R.H.S. A general correlation for flow boiling in tubes and annuli, *Int. J. Heat and Mass Transfer* 29 (1986), 351-358.
- [6] Jatuporn Kaew-On, Experimental investigation of evaporation heat transfer coefficient and pressure drop of R410A in a multiport mini-channels. *International Journal of Refrigeration* 32 (2009), 124-127.
- [7] Kim, Y. Seo, K. Chung, J.T. evaporation heat transfer characteristics of R410A in 7 and 9.52 mm smooth/micro-fin tubes, *Int. J. Refrigeration* 25 (2002), 716-730.
- [8] Lockhart, R.W. Martinelli, R.C. Proposed correlation of data for isothermal two-phase two-component flow in pipes, *Chem. Eng. Prog.* 45 (1945), 39-45.
- [9] Park, C.Y. Hrnjak, P.S. CO₂ and R410A flow boiling heat transfer, pressure drop, and flow pattern at low temperatures in a horizontal smooth tubes. *International Journal of Refrigeration* 30 (2007), 166-178.
- [10] Yun, R., Heo, J.H., Kim, Y., Evaporative heat transfer and pressure drop of R410A in micro-channels. *International Journal of Refrigeration* 29 (2006), 92-100.

Civil Engineering Article
/
İnşaat Mühendisliği Makalesi